

A Comparative Study of the Effect of Cavity and Obstacle on Propagation Behavior of Premixed Methane–Air Flame

Deyao Wu, Tianbao Ma, Jian Li*

State Key Laboratory of Explosion Science and Technology, Beijing Institute of Technology
Beijing, China

1 Introduction

Fire accident has always posed the risk of a major disaster in the chemical and mining industries [1,2]. Understanding the effect of the structural configuration on premixed flame propagation in ducts is of significance in devising strategies for mitigating such accidental explosions. Among these structural configurations, obstacles have always been the research focus. The effects of their fundamental parameters, including the blockage ratio, location, shape, number, spacing, arrangement, and obstacle properties, have been widely investigated [3]. Additionally, many studies have focused on premixed flame propagation in straight ducts, variable cross-section ducts, and bifurcation ducts [4–6]. However, the effect of a cavity on the propagation behavior of a premixed flame, a widely occurring phenomenon in mine and utility tunnels, has not been fully explained.

In this abstract, the propagation of a premixed methane–air flame in a duct with a cavity was experimentally investigated, and experiments in the obstructed duct were also conducted for comparison. We focus on the effect of obstacle and cavity on flame evolution and corresponding flame velocity and pressure. In addition, the different mechanisms of cavity and obstacle on flame propagation were also studied.

2 Experimental details

Figure 1 presents a schematic of the experimental apparatus, which comprises a combustion chamber, a gas distribution system, an ignition system, a high-speed camera, a pressure-data acquisition system, and a synchronization controller. The steel combustion chamber's cross-sectional area is 100 mm × 100 mm, and the chamber length is 1000 mm. As shown in Fig. 2, the cavity and obstacle are installed inside the combustion chamber during the experiment. A rectangular quartz glass window was installed on the front side of the combustion chamber to provide an optical area of 300 mm × 800 mm for visualization. A high-speed camera was used to record the flame evolution at a sample rate of 2000 fps. The pressure histories were measured using three PCB piezoelectric sensors (Model No.113B24) arranged on the upper wall, namely P1, P2, and P3. In this study, a premixed stoichiometric methane–air mixture was used. In the experiment, the combustion chamber was first pumped to a pressure of less than 100 Pa, and then, the premixed methane–air mixture was charged into the combustion chamber to a pressure of

101 kPa. The premixed methane–air mixture was ignited via the igniter with an ignition energy of 6 J, and the pressure-data acquisition system and high-speed camera were triggered concurrently.

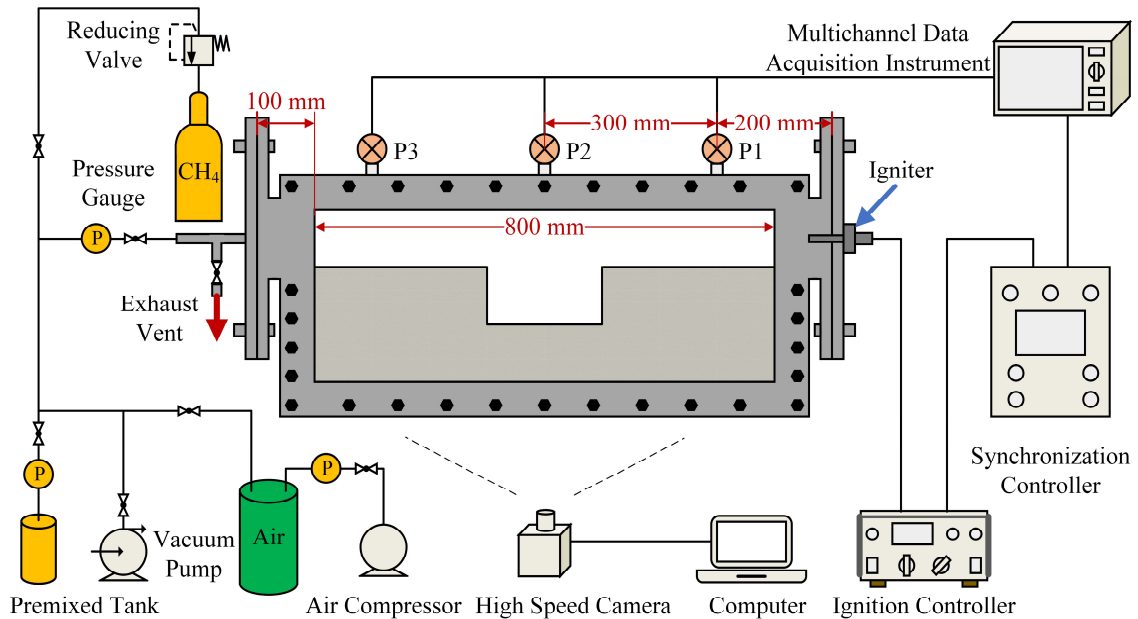


Figure 1 Schematic of the experimental apparatus.

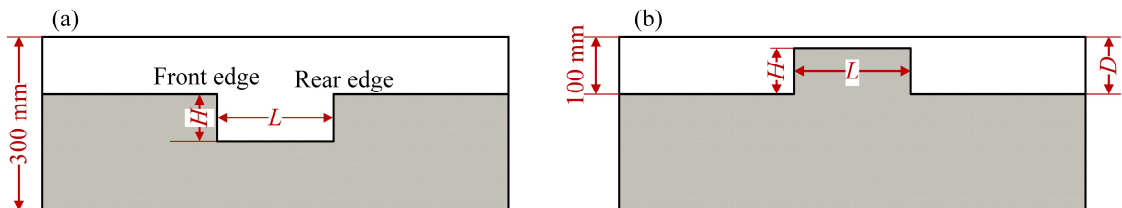


Figure 2 Schematic of (a) the cavity and (b) the obstacle.

3 Results and discussions

3.1 Flame morphology evolution and flame-tip dynamics

The cases with an obstacle/cavity of $L/D = 2$, $H/D = 0.5$ and 0.9 were taken as representative examples to compare the effect on the flame propagation behavior. Photographs of the premixed methane–air flame and the corresponding successive flame fronts are presented in Figs. 3–4, respectively. The lengths of the flame front obtained from the above sequential flame fronts were used to characterize the surface area of the flame front as shown in Fig. 5. The flame-tip velocity as a function of the flame-tip location (X) is illustrated in Fig. 6. As presented in Figs. 3–6, the flame evolution, flame front lengths and flame-tip velocity profiles can be divided into three stages considering the presence of the cavity/obstacle. Stage I involves the flame evolution upstream of the obstacle/cavity. At the early stage, the obstacle/cavity moderately affects flame evolution. Thus, the flame front length and flame-tip velocity profiles for the cases with a cavity are identical to that in the obstructed duct. Subsequently, the flame-tip velocity profiles diverge as the flame approaches the obstacle.

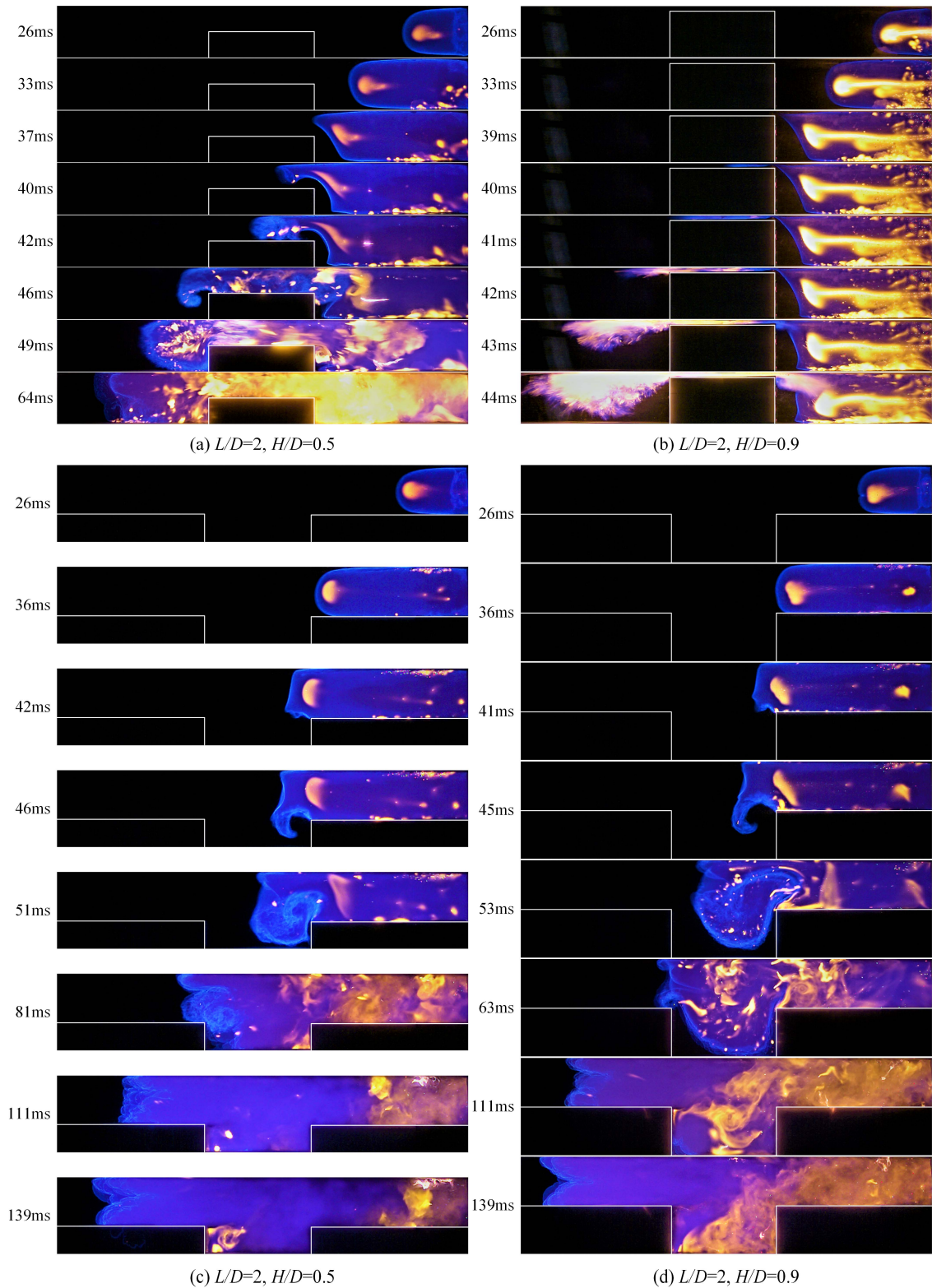


Figure 3 Comparison of flame morphology for cases of $L / D = 2, H / D = 0.5$ and 0.9 .

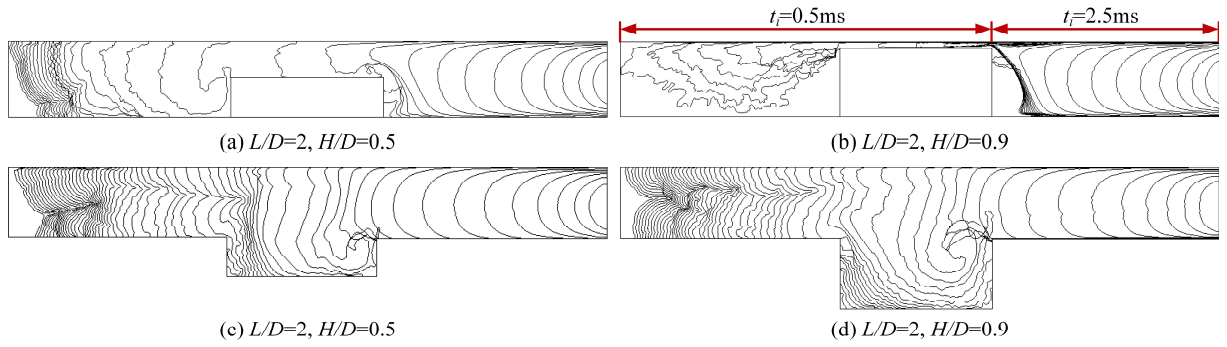


Figure 4 Comparison of successive flame fronts for cases of $L / D = 2$, $H / D = 0.5$ and 0.9 .

In stage II, the obstacle/cavity strongly affected the flame evolution and flame-tip velocity profiles by dictating the unburned gas flow filed ahead of the flame [7]. As presented in Figs. 3–5, for the cases with an obstacle, inclined flame and turbulent flame are successively formed in the gap between the obstacle and the upper wall of the duct. In contrast, the flame evolves into a vortex in the cavity for the cases with a cavity. However, the flame front lengths for cases with an obstacle/cavity are essentially identical. Thus, the velocity difference is mainly attributed to changes in the velocity of unburned gas flow ahead of the flame resulting from a sudden variation in the cross-section of the duct.

The flame evolution downstream of the obstacle/cavity was defined as stage III, and a more vital turbulent flame was induced by the obstacle in this stage, as demonstrated in Figs. 3–4. Correspondingly, the flame front length (L_f) in the obstructed duct is more significant than that in the duct with a cavity, as characterized in Fig. 5, thereby resulting in a significantly higher flame-tip velocity in the obstructed duct than in the duct with a cavity.

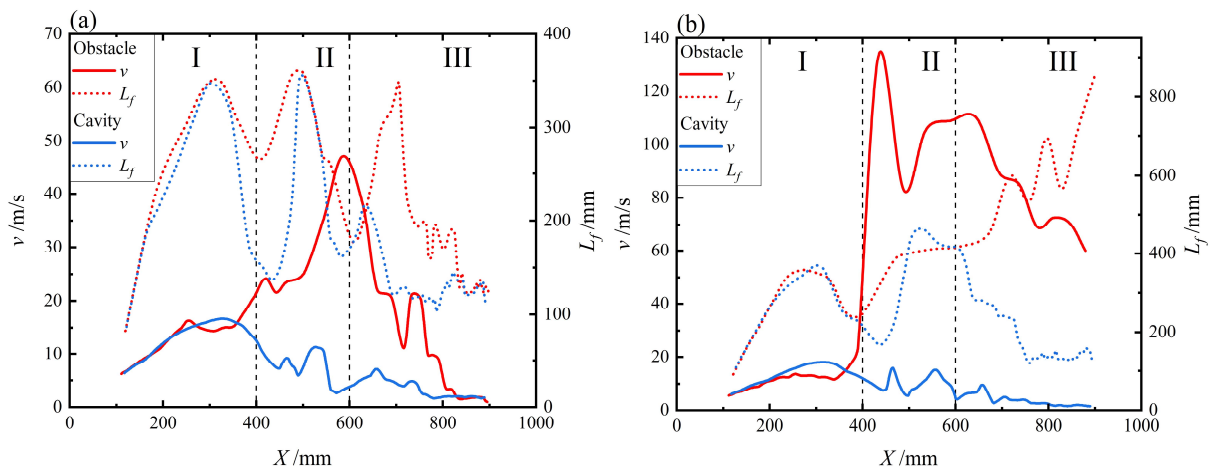


Figure 5 Comparison of flame-tip velocity and flame front length for cases of (a) $L / D = 2$, $H / D = 0.5$ and (b) $L / D = 2$, $H / D = 0.9$.

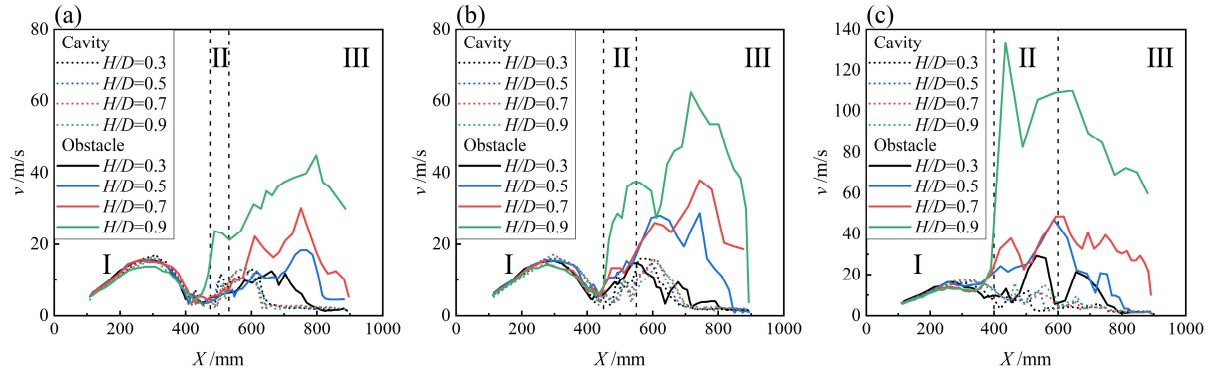


Figure 6 Flame-tip velocity versus location for cases: (a) $L/D = 0.5$, (b) $L/D = 1$ and (c) $L/D = 2$.

3.2 Pressure dynamics

Figure 7 compares the maximum pressure (P_{max}) in both the obstructed duct and the duct with a cavity. The P_{max} in the obstructed duct is larger when the H/D of the obstacle/cavity is identical, except for the cases with $L/D = 2$, $H/D = 0.3$ and 0.5 . This phenomenon is caused by the competition between the increased burning rate resulting from the stronger turbulent flame induced by the obstacle and the reduced fuel because of the decrease in combustion chamber volume due to the presence of an obstacle.

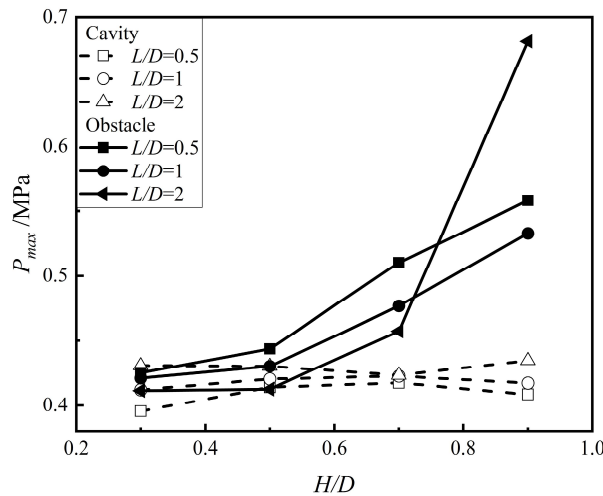


Figure 7 Maximum pressure (P_{max}) for cases featuring an obstacle/cavity.

Figure 8 shows the rate of pressure rise (dP/dt) versus time in the duct with an obstacle/cavity. As indicated by the trend in Fig. 8, when the H/D of the obstacle/cavity is identical, the maximum rate of pressure rise in the obstructed duct is larger than that in the duct with a cavity. In a closed combustion chamber, dP/dt depends mainly on the relationship between the heat-release rate and the heat-loss rate [8]. Presumably, the heat-release rate is affected by both the gas reactivity and flame surface area [9]. For all the cases considered in the present study, the heat-release rate depended solely on the flame surface area because all the experiments were performed using the same premixed methane–air mixture at a stoichiometric fuel/air ratio. During the flame evolution, the turbulent flame induced by the obstacle is stronger than that induced by the cavity. Therefore, the flame surface area in the obstructed duct is improved as shown in Fig. 5, thereby resulting in a larger maximum rate of pressure rise.

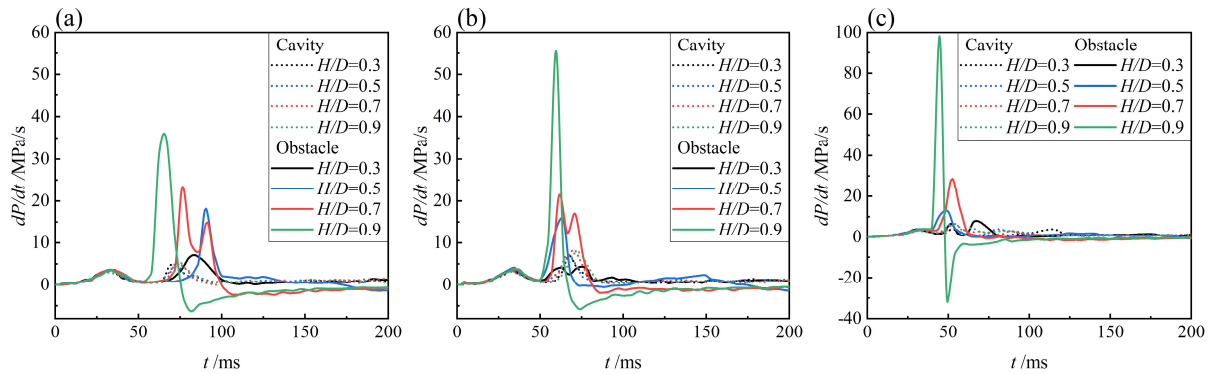


Figure 8 Rate of pressure rise versus time for cases: (a) $L/D = 0.5$, (b) $L/D = 1$, and (c) $L/D = 2$.

4 Conclusions

By comparing the flame propagation behaviors in the obstructed duct and the duct with the cavity, the results revealed that a higher flame-tip velocity and rate of pressure rise were obtained in the obstructed duct, resulting from the stronger turbulent flame induced by the obstacle. In addition, owing to the sudden decrease in the cross-section of the obstructed duct, the increase in the velocity of the unburned gas flow ahead of the flame contributed to the increase in the flame-tip velocity.

References

- [1] Bai C, Chang X, Zhang B. (2020). Impacts of turbulence on explosion characteristics of methane–air mixtures with different fuel concentration. *Fuel*. 271:117610.
- [2] Zheng L, Li G, Wang Y, et al. (2018). Effect of blockage ratios on the characteristics of methane/air explosion suppressed by BC powder. *J Hazard Mater*. 355:25–33.
- [3] Ma T, Wu D, Li J. (2023). Experimental study of the effect of a cavity on propagation behavior of premixed methane–air flame. *Fuel*. 338: 127341.
- [4] Wang J, Wu Y, Zheng L, et al. (2020). Study on the propagation characteristics of hydrogen/methane/air premixed flames in variable cross-section ducts. *Process Saf Environ*. 135:135–43.
- [5] Lin B, Guo C, Sun Y, et al. (2016). Effect of bifurcation on premixed methane-air explosion overpressure in pipes. *J Loss Prevent Proc*. 43:464–70.
- [6] Xiao H, He X, Duan Q, et al. (2014). An investigation of premixed flame propagation in a closed combustion duct with a 90° bend. *Appl Energ*. 134:248–56.
- [7] Johansen C, Ciccarelli G. (2009). Visualization of the unburned gas flow field ahead of an accelerating flame in an obstructed square channel. *Combust Flame*. 156:405–16.
- [8] Yang X, Yu M, Zheng K, et al. (2019). A comparative investigation of premixed flame propagation behavior of syngas-air mixtures in closed and half-open ducts. *Energy*. 178:436–46.
- [9] Yang X, Yu M, Zheng K, et al. (2020). An experimental study on premixed syngas/air flame propagating across an obstacle in closed duct. *Fuel*. 267:117200.